Research Article

Journal of Environmental Nanotechnology

Investigation on the Mechanical and Morphological behavior of Vetiver Fiber-reinforced Epoxy Composites with Nano-alumina Particles

N. Devendran*, T. S. Lakshmi and M. K. Muniyasamy

Department of Civil Engineering, Saveetha School of Engineering, Saveetha Institute of Medical and Technical Sciences, Chennai, TN, India

Received: 12.06.2025 Accepted: 28.06.2025 Published: 30.06.2025

*nmdev24@gmail.com

ABSTRACT

Light materials including fiber-reinforced polymer matrix are ideally suited to meet the contemporary demands for low-density materials with good mechanical strength. This initiative resulted in multiple studies aimed at integrating lignocellulosic natural fibers into polymer matrix. This work proposed the utilization of vetiver fibers (VF) (*Chrysopogon zizanioides*) as the reinforcement in epoxy composite integrated with nano alumina (nAl_2O_3) particles. Their mechanical properties were characterized by tensile, compression, flexural, and impact tests. Morphological investigations of VF-reinforced composite were performed to study fracture surfaces post-testing. Findings revealed a notable disparity upon the integration of nAl_2O_3 into the epoxy matrix. The impact tests showed superior performance in specimen with nanocomposite compared to the control group, with a mean value of 118 ± 2.9 J. Most mechanical properties in composites showed statistically significant improvements as confirmed by Tukey's test. SEM micrographs showed a significant reduction in agglomerations of nAl_2O_3 reinforcement and interface delamination, suggesting enhanced interface strength.

Keywords: Vetiver fibers; Alumina; Mechanical tests; Flexural strength; Epoxy composites.

1. INTRODUCTION

Plant-derived natural fibers were reviewed for their structural, thermal, mechanical, and chemical properties. Focus was placed on extraction methods, chemical treatments, and potential applications in sustainable bio-composites. Nautiyal *et al*. (2025) emphasized the biodegradability, recyclability, and eco-friendly usage of the fibers in the composite development. Natural fiber reinforced composites using raw natural fibers and polymer matrices were reviewed for their environmental, mechanical, and energy-saving benefits. Tyagi *et al*. (2024) analyzed parameters such as mechanical, thermal, and tribological behavior and their role in reducing pollution. These composites found applications in construction, biomedical, pharmaceutical, and furniture sectors due to their sustainable advantages. Senthilkumar *et al*. (2024) developed epoxy composites using hybrid luffa waste and groundnut shell fibers with varying Al_2O_3 filler contents (5–15 vol.%). The optimal mechanical and physical properties were observed for 30% hybrid fibers and 10% Al_2O_3, showing enhanced tensile, impact, flexural, shear strength, and hardness. XRD and surface morphology analyses validated the effective synergy among filler, fibers, and matrix, making them suitable for low-to-medium load applications Vetiver fiber (VF) and red mud were used as reinforcements in epoxy resin to fabricate five composites by hand lay-up with different wt %. Mechanical (tensile: 51.78 MPa, flexural: 35.92 MPa, impact: 29 kJ/m²) and thermal properties (*via* TGA) were studied alongside FTIR, XRD, and SEM analysis (Jena *et al*. 2022). Banana fiber-reinforced epoxy composites with fillers Al_2O_3 and boiled eggshell were fabricated with varying fiber lengths (100–200 mm) and filler loadings (5–15 wt%). Mechanical properties like tensile (14.25 MPa), impact (37.71 kJ/m²), and flexural strength (36.07 MPa) were optimized using Design Expert 13 and response surface methodology (Sathiyamurthy *et al*. 2023). Ramie, bamboo, and ramie-bamboo hybrid fiber composites within nano-SiC and nano-Al_2O_3 fillers were fabricated by hand layup and compression molding. The hybrid composite achieved highest tensile (50.16 MPa), impact (6.30 kJ/m²), and hardness (79.4), while pure ramie had the best flexural strength (101.4 MPa) (Kumar *et al*. 2025).

Polypropylene composites reinforced with 10 wt% NaOH-treated flax fiber and nano-Al_2O_3 (0–7.5 wt%) were fabricated using injection molding. Mechanical strengths, including yield (42.8 MPa), tensile (49.5 MPa), impact (18 J/mm²), and flexural (56 MPa) peaked at 7.5 wt% Al_2O_3. Manalu *et al*. (2024) examined the effect of compression molding pressure (10–30 MPa) on eco-friendly composites made from epoxy resin, rice husk, Al_2O_3, and Fe_2O_3. Among all samples, the BP10 (10 MPa) specimen achieved optimal density (1.881 g/cm³), hardness (80.5 Shore D), and flexural strength

(35.84 MPa). Venkatesh *et al*. (2024) developed a hybrid nanocomposite based on high-density polyethylene (HDPE) reinforced with 20 vol% chopped bast fiber and nano-Al_2O_3(2–6 vol%) using hand layup and thermal compression methods. The best properties were observed at 6 vol% Al_2O_3 with tensile strength (48 ± 2 MPa), hardness (45 HV), and low moisture absorption (7%). Krishnasamy *et al*. (2025) explored hybrid composites of curauá (C) and basalt (B) fibers in a polyester matrix, focusing on varying fiber lengths (4, 8, 12 mm) and loadings (25–75%). An 8 mm fiber length was found optimal; 75:25 B:C showed highest tensile (34.34 MPa) and flexural strength (119.6 MPa), while 25:75 B:C had best impact strength (60.12 kJ/m²)

Natural fibers derived from corn cob and palmyra fruit were used to fabricate composites by hand lay-up and Taguchi L9 orthogonal array design. The 12 mm thick composite achieved maximum impact strength (4.67 J/cm²); 10 mm thickness yielded Rockwell hardness (54) and tensile strength (23.31 MPa). ANOVA identified fiber weight percentage and thickness as key factors; regression showed <2% error, proving potential for eco-friendly decorative and disposable applications (Firoz *et al*. 2025).

Rout *et al*. (2025) analyzed hybrid NaOH-treated human hair, *Luffa cylindrica* fibers, and Incense Stick Ash (ISA) in composites using ultrasonication-assisted hand lay-up. The 10 wt% ISA composite had optimal mechanical properties (tensile: 19.04 MPa, impact: 39.6 J/cm²) and microhardness (22.3 Hv). TGA, ANOVA, and Whale Optimization Algorithm were used for wear behavior analysis, identifying abrasive and fatigue wear as dominant. Wear resistance was optimized through gray relational analysis based Whale Optimization Algorithm. Balasubramanian *et al*. (2025) developed vinyl ester composites reinforced within the 40 vol.% agave fiber and 1–4 vol.% porous biocarbon (from *Artocarpus hirsutus* husks), fabricated by hand lay-up. The results showed excellent mechanical, thermal, and dielectric properties, making the composite suitable for EMI shielding in electronics and communication devices.

Reddy *et al*. (2022) investigated natural fibers (*Abutilon indicum*, *Luffa cylindrica*, *Prosopis juliflora*) with NaOH, KOH, and silane treatments, and fillers ($CaCO_3$, Al_2O_3, TiO_2) in polymer composites. Silane-treated fibers and filler-loaded composites showed superior mechanical and wear properties, confirmed through SEM and FTIR. The Performance Selection Index helped identify the optimal hybrid combinations for challenging environments (moisture, temperature, chemical exposure). Aynalem and Sirahbizu, (2021) investigated chopped flax fiber–unsaturated polyester resin composites reinforced with Al_2O_3 fillers (0–15 wt%) by hand lay-up and compression molding. The 25 wt% flax/5 wt% Al_2O_3 composite showed a 39.06% increase in tensile strength, and 15 wt% flax/10 wt% Al_2O_3 composite showed a 45% increase in impact strength.

Hybrid bio-composites were fabricated utilizing short sugarcane fibers (SCF) and tamarind seed powder (TSP) in epoxy resin by hot injection molding. The 35 wt% SCF/15 wt% TSP composition achieved the highest flexural strength (36.543 MPa) and compressive strength (21.32 MPa). Proper balancing of fiber and filler contents was crucial for enhanced mechanical behavior (Girimurugan *et al*. 2022b). Ben *et al*. (2021) developed an areca fiber-reinforced epoxy biocomposite toughened with neem oil and nano-silica (2 vol.%), all surface-treated with aminopropyltriethoxysilane. The composite showed high storage modulus (9.8 GPa at room temp), better glass transition, and enhanced antimicrobial properties. The composite was suitable for food packaging, medical carriers, and domestic appliances due to combined mechanical and antibacterial performance.

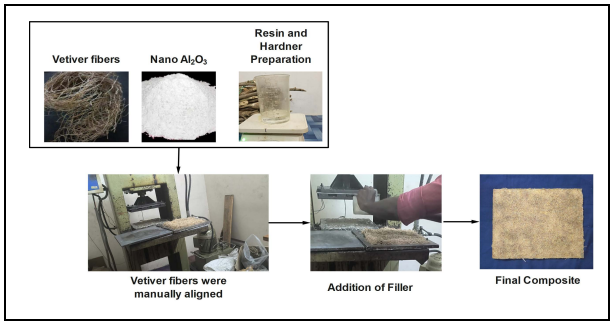


Fig. 1: Fabrication of the composite specimen

Girimurugan *et al*. (2022a) developed polypropylene-based hybrid polymer composites utilizing nano alumina and water hyacinth stem powder, fabricated by injection molding. The aim was to improve mechanical strength, especially tensile properties, by varying the nano alumina content. All samples were tested per ASTM standards, showing notable tensile enhancement due to nano alumina addition. Thangaraj *et al*. (2022) studied HDPE composites that were reinforced with nano alumina and areca nut shell powder in varied ratios to improve tensile, compressive, and yield strengths. The best performance (tensile: 49.37 MPa, compressive: 46.71 MPa) was achieved with 2.5 wt% nano alumina + 7.5 wt% areca nut shell powder. This hybrid composite was proposed as a sustainable alternative to wood-based materials. Eco-friendly hybrid composites were prepared using Areca (ARF) and Abaca (ABF) fibers with epoxy resin and nano-silica (SiO_2) as filler. The optimal composition (76% ABF, 20% ARF, 4% nano-SiO_2) showed enhanced tensile, flexural, and impact strength, along with reduced environmental impact. The SEM analysis confirmed strong fiber–matrix bonding and reduced delamination (Harak *et al*. 2024).

The current study aimed to evaluate the mechanical properties of epoxy composites reinforced with up to 25% vetiver (*Chrysopogon zizanioides*) fibers and functionalized with Al_2O_3. The mechanical performance was evaluated by Impact, tensile, flexural, and compression tests. To further understand how the composite fractured, SEM was employed to analyze the fractured surfaces. The objective of this study is to find out whether the Al_2O_3 treatment improves mechanical performance and, by extension, the interaction between fibers and the matrix.

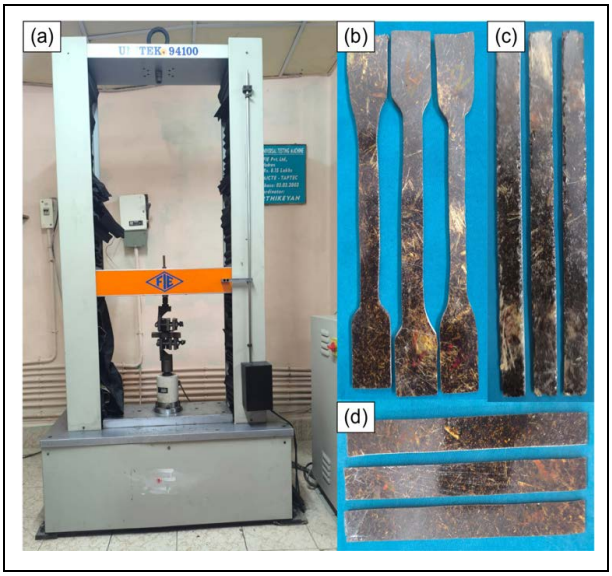


Fig. 2: (a) Universal testing machine and specimens for (b) tensile test, (c) compression test and (d) flexural test

2. MATERIALS AND METHODOLOGY

2.1 Materials

This research utilized an epoxy resin (LY556) and hardener (HY951), obtained from Kovai Cheenu Enterprises, Coimbatore, Tamil Nadu, India. The nano-Al_2O_3 utilized in this study was supplied by Matrics Enterprises, Nagercoil, Tamil Nadu, India. The nanomaterial was incorporated in the epoxy resin by drying 25 mL suspension of nAl_2O_3 until it reached 2 wt% concentration in the resin, ensuring complete removal of water. To make a uniform solution of Al_2O_3 in alcohol, 50 mL of isopropyl alcohol was added to the dried Al_2O_3 suspension, followed by addition of 100 g of epoxy resin. The epoxy/Al_2O_3 mixture was mixed using a mechanical shaker. This mixture was then heated at 80°C for one day to evaporate isopropyl alcohol, minimizing the risk of air void formation during curing. The matrix material for the composites was then fabricated by adding the hardener to the epoxy/Al_2O_3 suspension (Fig. 1).

Vetiver fibers were sourced from multiple sites in Erode, Tamil Nadu, India. The roots were initially cleansed by hand and subsequently submerged in pure water for one day to improve their pliability and ease the defibration process. Fiber extraction was performed manually with a sharp stiletto to meticulously detach the fibers from their roots. The retrieved fiber bundles were first cut to a length of approximately 100 mm and subsequently desiccated in oven at 75 °C for one day. No chemical treatment was applied to these fibers. Additionally, the dry fiber bundles were trimmed to a 50 mm length prior to composite manufacturing.

2.2 Processing of the Composite Materials

The vetiver fibers were carefully arranged in a 250 × 200 × 3 mm metal mold to create the composite plates. The fibers were aligned and placed in the mold chamber according to a specific ratio of fibers to resin (Bothiraj *et al*. 2022). Using geometric linear density method, 100 fibers were weighed. Their diameter and length were measured under an optical microscope for calculation purposes. On an average, 0.46 g/cm^3 was found to be the density of vetiver fiber. The epoxy resin has a density of 1.12 g/cm^3. Up to 25% VFs were incorporated into neat epoxy and Al_2O_3 /epoxy plates. The next step was to cure them at room temperature (RT) by subjecting them to processing at a pressure of 5 tons for 24 hours.

Table 1 shows the composition percentages of the fabricated composites.

Table 1. Compositions of the fabricated composites

S. No.	Specimen Code	Epoxy	Vetiver Fiber	Al_2O_3 Filler
1	S_1	100	-	-
2	S_2	85	15	
3	S_3	80	20	
4	S_4	75	25	
5	S_5	73	25	2

2.3 Tensile Tests

For tensile testing, three samples were taken from the composite plates. The 90 mm gauge length and 150 mm × 15 mm × 2 mm dimensions were specified in the ASTM D3039/2014 standard. A FIE – Universal Testing Machine (UTM) with the capacity of 5 kN and 2 mm/min crosshead speed was utilized to conduct the experiments at room temperature (Fig. 2a, 2b).

2.4 Compression Tests

The FIE-UTM was utilized to conduct compression tests at room temperature in compliance

with ASTM requirements. Vetiver fibers were surface-modified (e.g., benzoylation) to improve compatibility with polymer matrices. Parameters such as mechanical and thermal properties were analyzed using FTIR, XRD, and SEM. Benzoylation-treated fibers showed the best performance among treatments, enhancing fiber–matrix interaction (Jena *et al.* 2022). A 2 mm/min crosshead velocity was employed. Three identical specimens were fabricated within the dimensions of 100 mm × 12 mm × 3 mm (Fig. 2c).

2.5 Flexural Tests

Flexural tests are conducted utilized a FIE - UTM at room temperature and a crosshead speed of 2 mm/min. Composite plate specimens were machined and sectioned based on ASTM D790 standards (Amjad *et al.* 2021). For every percentage of fiber, three samples were made with dimensions of 100 × 12 × 3 mm (Fig. 2d).

2.6 Impact Tests

Three specimens from composite were machined from the composite plates for the Izod impact tests, adhering to the parameters outlined in the ASTM D256/2018 standard (Tavadi *et al*. 2025). The impact tests were conducted using a 22J hammer on a type XC-50 Pantec equipment at room temperature.

2.7 Scanning Electron Microscope (SEM)

A ZEISS FE-SEM model setup was used to study the fractured surfaces of the composite. The set was operated between 9 to 10 kV and a secondary electron detector. To generate an electron current, the fibers were coated with gold using sputter coater. This allows for the examination of micrographs showing the failure mechanisms with improved resolution and few artifacts (Jha *et al*. 2022).

2.8 Statistical Analysis

Tensile, flexural and impact results were compared using ANOVA. F-test was used to identify statistically significant variations and Tukey honestly significant difference (HSD) test was used for pairwise comparisons of means for every group (Dos *et al*. 2024).

$$HSD = q\sqrt{\frac{EMS}{r}} \quad \ldots (1)$$

3. RESULTS AND DISCUSSION

3.1 Analysis of Tensile Strength

Fig. 3 illustrates the mean tensile strength for all the fine specimens. The novel hybrid nanocomposite exhibited superior tensile strength relative to the vetiver-reinforced composites, likely due to the homogenous dispersion of Al_2O_3 inside the epoxy matrix and enhanced interfacial bonding. Nevertheless, S_5 state demonstrates low tensile properties compared to S_1. This might be because the fibers were not able to provide enough reinforcement when the materials were subjected to tensile loads. So, the fibers probably compromised the fiber/matrix interface by acting as structural flaws in the material.

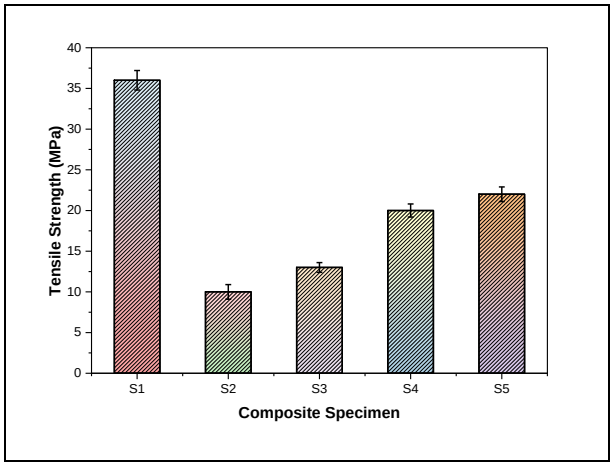


Fig. 3: Tensile strength of fabricated composites

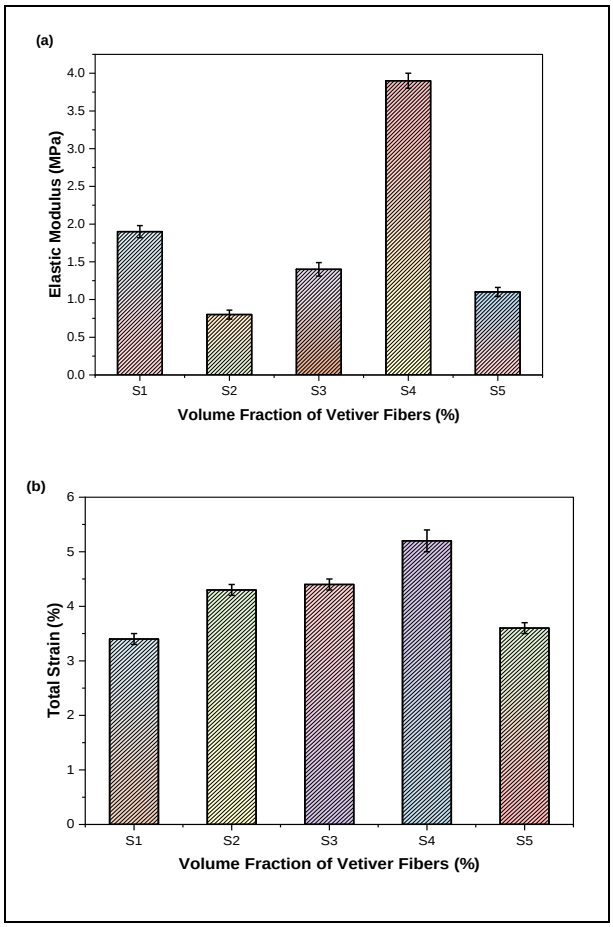


Fig. 4: Vetiver fiber volume fraction *vs* (a) elastic modulus (b) strain of S_1 to S_5 conditions for tensile strength

The micrographs clearly display the cracks that developed during the process. Fig. 5a shows a cluster of Al_2O_3 nanoparticles, which could affect the mechanical properties with an increase in interfacial resistance due to ionic interactions and hydrogen bonds Fig. 5b shows the river markings, indicating the possibility of a brittle fracture. The pullout mechanism is evident with severed fibers and no signs of delamination. Fig. 4 illustrates a trend of rising elastic modulus in composites solely reinforced with vetiver fibers, perhaps due to the superior stiffness of the fibers. Conversely, the specimen S5 did not exhibit the similar tendency, likely due to its elevated aspect ratio and the decreased mobility of the polymeric chains resulting from the interaction with nAl_2O_3. Conversely, total strain graph indicates that reinforcements exhibit no substantial change across the various conditions examined within the standard deviation.

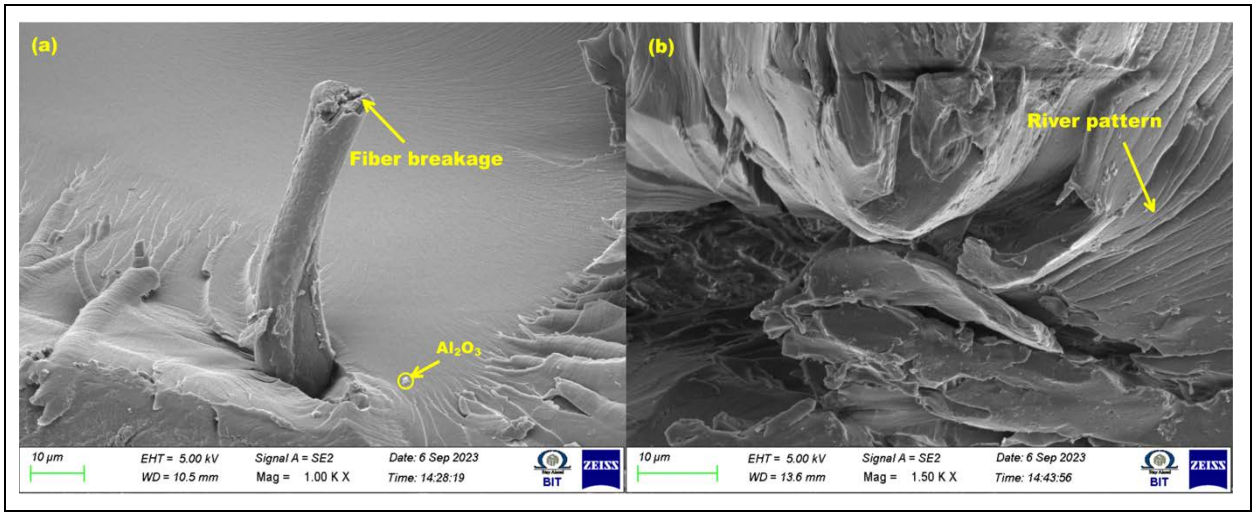


Fig. 5: SEM images of fractured surface after tensile test

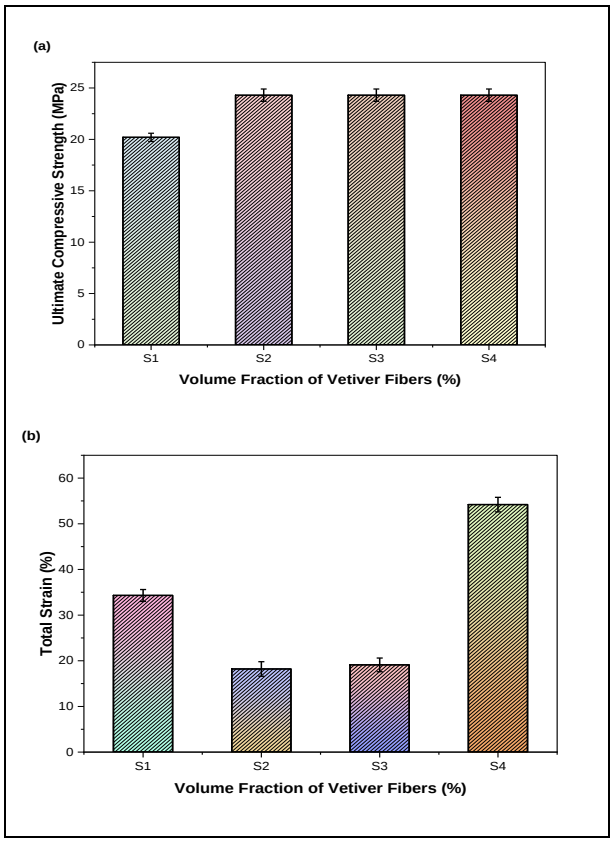


Fig. 6: (a) Compressive strength and (b) Total strain percentage of S_1 to S_4

Table 2 shows the analysis of variance for ultimate tensile strength (UTS) of the fabricated composites. The hypothesis of identical averages is rejected at a 5% significance level. Consequently, it was established that a substantial variance existed in the tensile strength among the various conditions of the vetiver composites.

Table 2. ANOVA of the UTS for composites S_1, S_2 to S_4, and S_5

	DF	Sum of Squares	Mean Square	F Value	Prob>F
Model	4	1226.4	306.6	109.5	<0.0001
Error	10	28	2.8		
Total	14	1254.4			

Table 3. Variations in mean values of UTS by Tukey's test

	E	EV-15	EV-20	EV-25	EV-25
S_1	0	26	23	16	14
S_2	26	0	3	10	12
S_3	23	3	0	7	9
S_4	16	10	7	0	2
S_5	14	12	9	2	0

Table 3 provides the outcomes of Tukey test for ultimate tensile strength. The elastic modulus of 3.97 MPa and variations over this threshold are considered

significant. The results show that the S_5 condition outperformed all other examined groups. Similarly, FVL3 (flax + vetiver) had 65% balanced strength. (Sivanantham *et al*. 2025).

3.2 Analysis of Compressive Strength

The specimens were tested for their compressive stress and average maximum strain capacity (Fig. 6). Compressive stress under different reinforcing conditions is also compared. Both the ultimate compressive strain and the overall strain were highest in the S_5 condition. Better load transmission from the matrix to the fibers is associated with nAl_2O_3 presence because it improves interlock between the two. The compressive characteristics were considerably improved. Conversely, the pristine epoxy reinforced with untreated VFs may function as fillers. The S_2 to S_4 conditions exhibit ineffective load transfer, resulting in a final performance (mostly fragile), similar to that of S1.

Micrographs were analyzed to understand the events that caused the fracture. Fig. 7(a) illustrates the delamination of the epoxy matrix, accompanied by significant adhesion at the fiber/matrix bonding. Fig. 7 (b) illustrates crack propagation within the fiber, which may serve as a potential mechanism for fiber fracture initiation. Fig. 7(b) shows a river pattern process associated with crack development lacking a favoured orientation. It illustrates the occurrence of the pullout process and the curvature at the termini of the vetiver fiber.

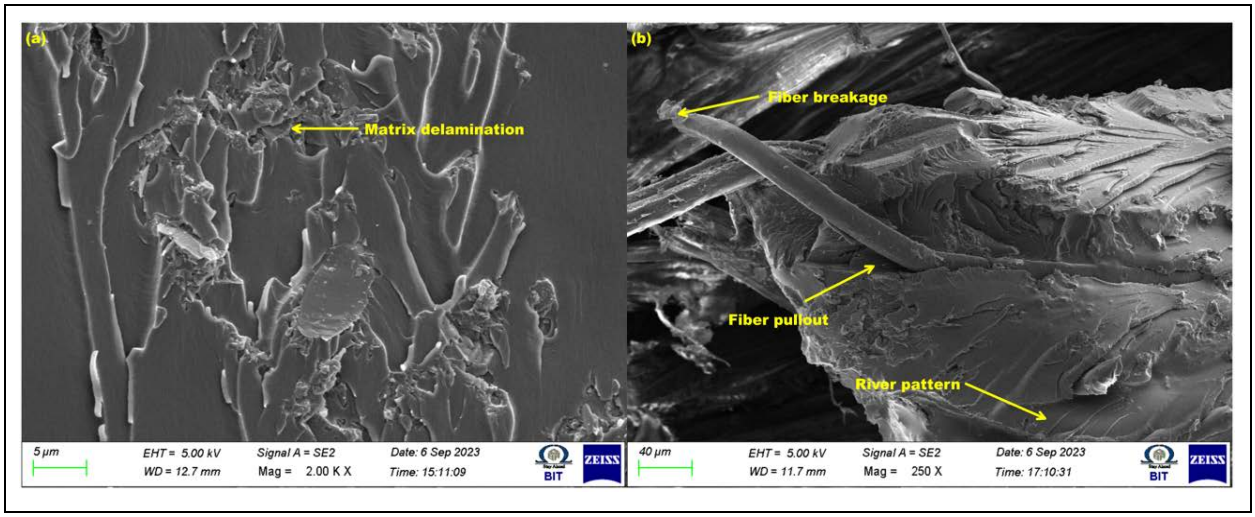


Fig. 7: SEM images of the fractured specimens after compression test

Table 4 presents the ANOVA findings for compressive stress under examined conditions to observe if a considerable difference exists among the outcomes. Given that the computed F value (8.93379) exceeds the prob F value (0.00621), one can conclude that the examined conditions influence the efficiency of the material under compressive stress.

Table 4. ANOVA of compressive stress for S_1, S_2 to S_4 and S_5

	DF	Sum of Squares	Mean Square	F Value	Prob>F
Model	3	37.9456	12.6485	8.93379	0.00621
Error	8	11.3265	1.41581		
Total	11	49.2721			

Tukey's test was employed to evaluate the average with 95% CI to determine the best results produced by the parameters. The determined value for HSD was 3.58 MPa (Table 5). The S_4 condition has a substantial disparity relative to the other conditions. This signifies that Al_2O_3 substantially enhanced mechanical performance. For this reason, the tensile test was the only mechanical evaluation where the nanocomposite failed to show a discernible improvement over the S_4 condition. But out of all the tests, only the impact tests outperformed the control group.

Table 5. Variations in mean values of CS by Tukey's test

	E	EV-15	EV-20	EV-25
S_1	0	3.81	3.58	3.46
S_2	3.81	0	0.23	0.35
S_3	3.58	0.23	0	0.12
S_4	3.46	0.35	0.12	0

The literature substantially indicates that inadequate dispersion of nanomaterials can be remedied with specific chemical changes to enhance the particle-matrixing (Janyakunmongkol *et al*. 2024). Consequently, it serves as a superior choice for enhancing the

mechanical performance of nanocomposites. Generally, they exhibit superior mechanical performance compared to nAl_2O_3, without requiring an increased percentage. This renders the alteration economically feasible while preventing undesired agglomerations.

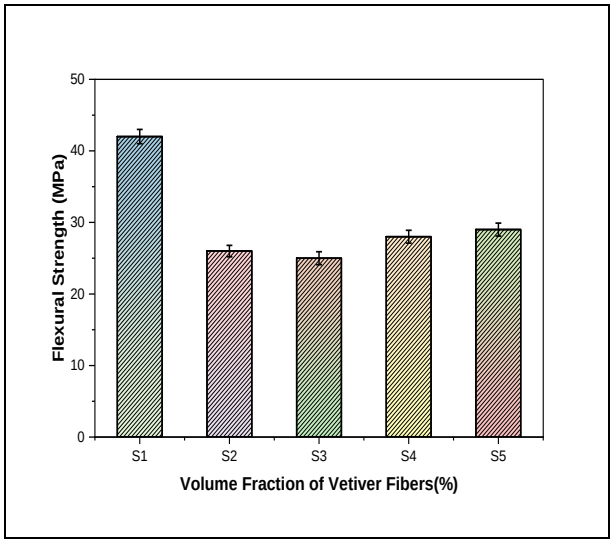


Fig. 8: Comparison of flexural strength for the various composites

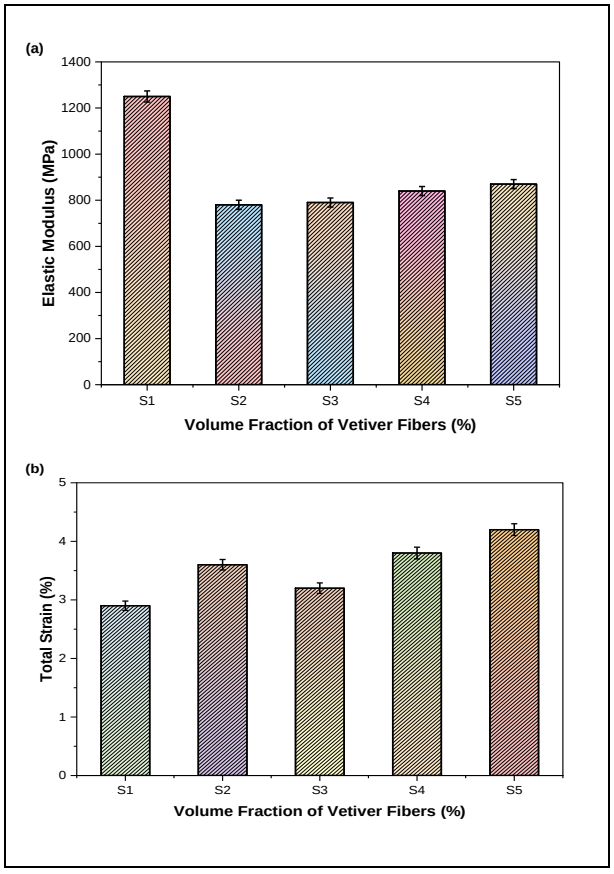


Fig. 9: Volume fraction of vetiver fibers *vs* (a) Elastic modulus (b) Total strain for flexural strength of various composites

Table 6. ANOVA of FS for the composites S_1, S_2 to S_4, S_5 nanocomposite

	DF	Sum of Squares	Mean Square	F Value	Prob>F
Model	4	570	142.5	89.0625	<0.0001
Error	10	16	1.6		
Total	14	586			

Table 7. Variations in mean flexural strength by Tukey's test

	E	EV-15	EV-20	EV-25	EV-25
S_1	0	15	16	13	12
S_2	15	0	1	2	3
S_3	16	1	0	3	4
S_4	13	2	3	0	1
S_5	12	3	4	1	0

3.3 Flexural Strength Analysis

Fig. 8 and 9 illustrate the averages and standard deviations of the mechanical parameters obtained from the flexural tests for S_1, composites upto S_4, and S_5 nanocomposite. The current investigation demonstrated an increasing tendency till S_5, as depicted in Fig. 8. Nevertheless, the S_1 condition exhibited superior mechanical performance regarding flexural strength and elastic modulus compared to all other examined conditions. The vetiver fibers functioning as a filler instead of reinforcement could be the cause of the decreased mechanical performance. Moreover, a deficient contact among the matrix and fiber may still serve as an indication. Ultimately, the potential formation of gaps between the fibers, resulting from the inability of the resin to adequately wet all fiber material, may signify areas that could function as stress concentrators.

The overall strain behavior is illustrated in Fig. 9. The results indicate that S_1 composites exhibit completely brittle property, while other composites show increased total strain. This improvement in ductility is attributed to the reinforcing effect of fibers and Al_2O_3 nanoparticles, which enhance the overall durability of the developed material. From S_3 to S_5, the elastic modulus showed an increasing trend when reported for all composite circumstances. This is probably due to the action of nAl_2O_3, which increases the material's hardness. SEM micrographs were acquired as shown in Fig.10 to understand the fracture mechanisms that result in the augmentation of the reinforcements under the test conditions. Fig. 10(a) exhibits brittle fracture characterized by the presence of river pattern and fiber to fiber ruptures. In S_3 condition, fiber-related fracture mechanisms become prevalent along with fiber delamination and cracking as illustrated in Fig. 10(b).

The latter occurs less often and may indicate delamination among the matrix and the fiber. The functionalization of the matrix with nAl_2O_3 clearly helped achieve a stronger interaction among the reinforcement and matrix phase.

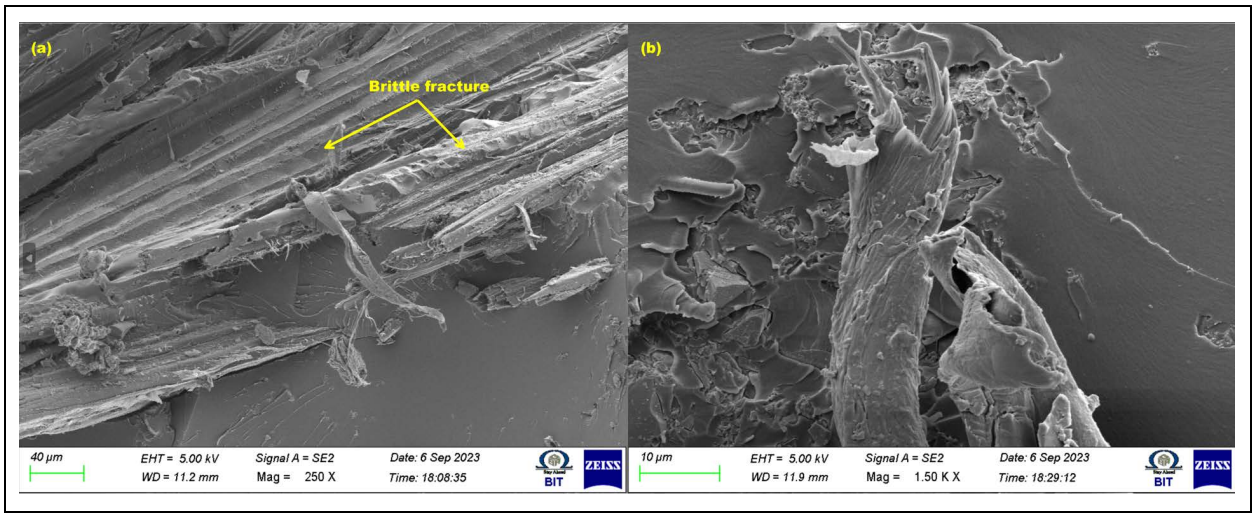


Fig. 10: SEM images of tensile strength fractured composites

ANOVA was conducted to observe the variation in flexural properties among the various groups. In Table 6, the hypothesis of equivalent mean is rejected at a 5% confidence level. This is attributed to the estimated F-value that exceeds the tabulated critical F-value. This suggests that a substantial variance exists in the flexural strength attribute across various reinforcement circumstances.

Table 7 shows the flexural strength findings of the Tukey HSD test. The values indicate that the S_1 condition outperformed all other examined composites. The S_5 is distinct from the other vetiver-reinforced composites.

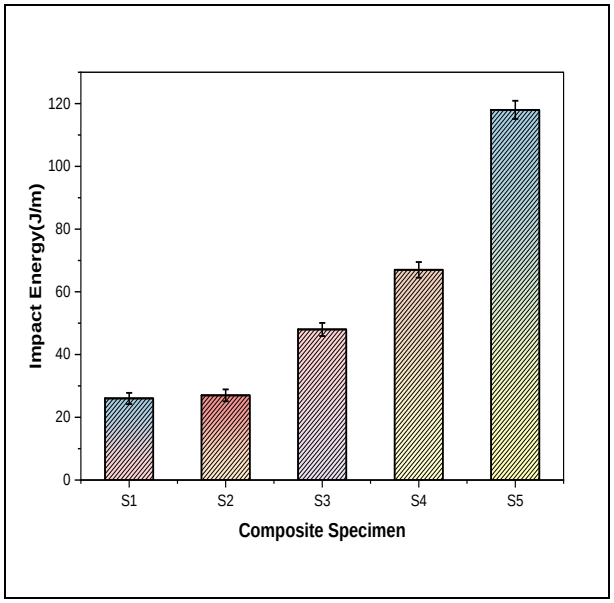


Fig. 11: Impact energy for the composite specimens

3.4 Izod Impact Analysis

Fig. 11 illustrates a correlation between elevated filler content and enhanced impact energy. The S_5 demonstrated a substantial increase of 480% compared to the S_1. A 153% rise was observed when comparing S_5 and S_4. The Izod impact characteristics have been altered by the incorporation of a new nAl_2O_3 phase that functionalizes the nanoparticle. Consequently, as previously shown microscopically, an increased density of river mark propagation along with a reduction in delamination at fiber interface/matrix, correlates with enhanced energy absorption.

An analysis of variance was performed to know if any considerable difference existed among average Izod impact outcomes. Table 8 illustrates that the hypothesis of equal means was rejected at 5% significance level, as the computed F-value exceeded the critical F-value. Thus, this verifies that a substantial disparity existed in the impact energy among various composites.

Table 8. ANOVA of impact energy for S1, S2 to S4 and S5 nanocomposites

	DF	Sum of Squares	Mean Square	F Value	Prob>F
Model	4	17288.4	4322.1	1964.59	<0.0001
Error	10	22	2.2		
Total	14	17310.4			

Table 9 presents the results of the Tukey HSD test to investigate variations in the mean impact energy. The computed HSD of 3.52 J/m indicated that the variations exceeding this value are deemed significant.

Only S_2 condition did not exceed the calculated HSD. The S_5 outperformed all other examined group circumstances.

Table 9. Variations in mean impact energy by Tukey's test

	S1	S2	S3	S4	S5
S_1	0	2	24	43	92
S_2	2	0	22	41	90
S_3	24	22	0	19	68
S_4	43	41	19	0	49
S_5	92	90	68	49	0

The fracture mechanism associated with fiber rupture is discernible at a macroscopic level. The Izod impact characteristics were modified as a result of EP-Al_2O_3 functionalization, introducing a new phase. As a result, new types of fractures were seen, which could improve energy absorption. Fig. 12 shows the micrographs that are relevant to the mechanisms of fracture.

All micrographs distinctly exhibit an enhancement at fiber-matrix interface, characterized by minimal presence of delamination fracture process. The delamination is attributed to inadequate fiber attachment due to the disparity in hydrophobic and hydrophilic properties. Nonwoven fibers outperformed woven ones, and cross-directional alignment provided superior strength (Senguptaa, 2020). Furthermore, the use of the Al_2O_3 nanofiller enhances the toughness and overall mechanical characteristics of the material, potentially contributing to the rise in impact energy. Additionally, fracture processes including tearing of fiber and pulling also exist. Fig. 12(a) shows the imprint and void of fiber on the matrix surface, while Fig. 12(b) demonstrates the presence of fiber tearing and river pattern.

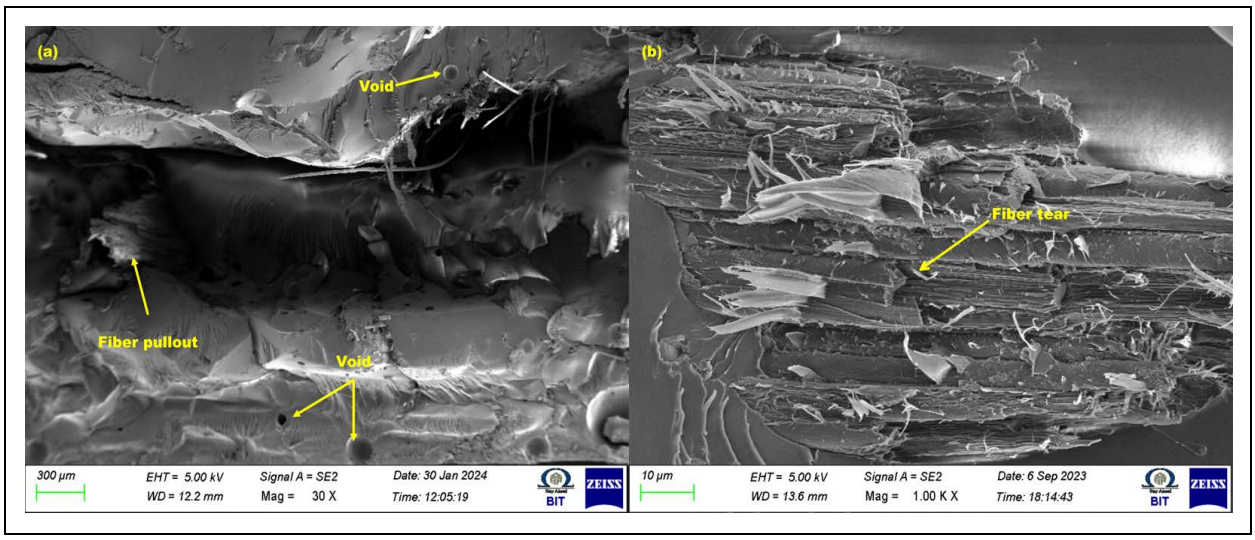


Fig. 12: SEM images of fractured S_4 composites

4. CONCLUSIONS

Among all assessments, only the impact tests showed superior performance in the S_5 condition compared to the control group, with a mean value of 118 ± 2.9. The tensile strength of the composites averaged 22 ± 0.9 MPa, showing no significant improvement over the S_4 condition. The average bending and compression strengths were 29 ± 0.9 MPa and 24.3 ± 0.6 MPa, respectively. Except for the TS, all other mechanical tests showed significant differences compared to the S4 specimens, as validated by Tukey's test. Scanning electron microscopy micrographs demonstrated the presence of agglomerations of the nano reinforcement. This delamination significantly diminished, suggesting a more robust interface. This probably enhanced the overall mechanical performance. Nonetheless, the agglomerations may have exerted a countervailing influence. Furthermore, ANOVA analysis revealed substantial disparities across the different conditions for mechanical tests conducted.

CONFLICTS OF INTEREST

The authors declare that there is no conflict of interest regarding the publication of this paper.

FUNDING

This research received no specific grant from any funding agency in the public, commercial, or not-for-profit sectors.

COPYRIGHT

This article is an open-access article distributed under the terms and conditions of the Creative Commons Attribution (CC BY) license (http://creativecommons.org/licenses/by/4.0/).



REFERENCES

Amjad, A., Abidin, M. S. Z., Alshahrani, H. and A Rahman, A. A., Effect of fibre surface treatment and nanofiller addition on the mechanical properties of flax/pla fibre reinforced epoxy hybrid nanocomposite, *Polym.*, 13(21), 3842(2021). https://doi.org/10.3390/polym13213842

Aynalem, G. F. and Sirahbizu, B., Effect of Al_2O_3 on the tensile and impact strength of flax/unsaturated polyester composite with emphasis on automobile body applications, *Adv. Mater. Sci. Eng.,* 2021(1), 6641029(2021). http://dx.doi.org/10.1155/2021/6641029

Balasubramanian, R., Khare, N., Mann, V. S., D, G. A. G. M., Masih, S. A., Nagarajan, N., Suresh, K. N. and Rao, P. G., Synthesis of Porous Biocarbon from Artocarpus hirsutus Husks and Its Microwave Shielding Effect on Agave Fiber-Reinforced Vinyl Ester Composite at High-Frequency Bands, *Fibers. Polym.*, 26(3), 1281–1296(2025). https://doi.org/10.1007/s12221-024-00832-w

Ben, S. J., Julyes, J. S., Sivakumar, K., Mayakannan, A. V. and Arunprakash, V. R., Visco-Elastic, Thermal, Antimicrobial and Dielectric Behaviour of Areca Fibre-Reinforced Nano-silica and Neem Oil-Toughened Epoxy Resin Bio Composite, *Silicon.*, 13(6), 1703–1712(2021). https://doi.org/10.1007/s12633-020-00569-0

Bothiraj, T., Boopathi, K., Kalaiselvan, K., Benham, A. and Mayakannan, S., Experimental investigations on mechanical and wear behavior of waste marble dust and coconut fiber reinforced hybrid bio composites, *Mater. Today. Proc.,* 68(6), 2239–2242(2022). https://doi.org/10.1016/j.matpr.2022.08.441

Dos, S. A. J. G., Ribeiro, M. M., Corrêa, A. D. C., Rodrigues, J. D. S., Silva, D. S., Junio, R. F. P. and Monteiro, S. N., Morphological, chemical and mechanical properties of hybrid polyester composites reinforced with bamboo fibers and kaolin waste, *J. Mater. Res. Technol.*, 30, 1–15(2024). https://doi.org/10.1016/j.jmrt.2024.03.003

Firoz, K. M., Alamgir, H. M., Abubakar, S. M. and Mosharraf, H. M., Investigate the effects of different control factors on mechanical characteristics of natural fiber reinforced composite, *Next. Mater.,* 8, 100608(2025). https://doi.org/10.1016/j.nxmate.2025.100608

Girimurugan, R., Sahoo, G., Sivalingam, A. and Mayakannan, S., Effect of nano alumina powder and water hyacinth stem powder addition on tensile properties of polypropylene matrix hybrid composites – An experimental study, *Mater. Today. Proc.*, 60(2), 2099–2104(2022a). http://dx.doi.org/10.1016/j.matpr.2022.01.477

Girimurugan, R., Shilaja, C., Mayakannan, S., Rajesh, S. and Aravinth, B., Experimental investigations on flexural and compressive properties of epoxy resin matrix sugarcane fiber and tamarind seed powder reinforced bio-composites, *Mater. Today. Proc.*, 66, 822–828(2022b). http://dx.doi.org/10.1016/j.matpr.2022.04.386

Harak, S. S., Krishnaveni, K., Karthick, K., Chinnarasu, K., Venkata, H. P. P., Tonk, A. and Mayakannan, S., Experimental Study on the Mechanical Properties of Hybrid Areca and Abaca Fiber Reinforced Polymer Composites, *J. Environ. Nanotechnol.*, 13(4), 92–101(2024). https://doi.org/10.13074/jent.2024.12.244977

Janyakunmongkol, K., Nhuapeng, W. and Thamjaree, W., Effect of alkaline treatment on mechanical properties of composites between vetiver fibers and epoxy resin, *J. Mech. Behav. Mater.,* 33(1), 20220310(2024). https://doi.org/10.1515/jmbm-2022-0310

Jena, P. K., Mohanty, J. R. and Nayak, S., Effect of Surface Modification of Vetiver Fibers on Their Physical and Thermal Properties, *J. Nat. Fibers.,* 19(1), 25–36(2022). https://doi.org/10.1080/15440478.2020.1726249

Jena, P. K., Mohanty, J. R., Nayak, S., Khuntia, S. K., Panda, K. R. and Sahu, R., Comprehensive investigation of mechanical and thermal properties of vetiver grass and red mud reinforced hybrid composites, *J. Nat. Fibers.,* 19(13), 5152–5162(2022). https://doi.org/10.3390/bdcc7010025

Jha, K., Tamrakar, P., Kumar, R., Sharma, S., Singh, J., Ilyas, R. A., Rangappa, S. M. and Siengchin, S., Effect of hybridization on physio-mechanical behavior of Vetiver and Jute fibers reinforced epoxy composites for structural applications: Studies on fabrication, physicomechanical, water-absorption, and morphological properties, *J. Ind. Text.*, 51(2), 2642-2664(2022). https://doi.org/10.1177/15280837221098573

Krishnasamy, S., Irulappasamy, S., Thiagamani, S. M. K., Ilyas, R. A. and Khoo, P. S., Examining the mechanical properties of hybrid curauá-basalt reinforced polyester composites, *Polym. Compos.,* 29694(2025). https://doi.org/10.1002/pc.29694

Kumar, K. P., Lokeshwar, G., Reddy, C. U. K., Shetty, N., Shahabaz, S. M. and Nargis, T., Experimental investigation of mechanical properties and morphology of ramie, bamboo, and ramie-bamboo hybrid composites with silicon carbide and alumina nano-fillers, *Mater. Res. Express*., 12(2), 025306 (2025).

Manalu, J., Numberi, J. J., Safanpo, A., Fitriyana, D. F., Wijaya, T. L., Siregar, J. P., Cionita, T. and Jaafar, J., Characterization of eco-friendly composites for automotive applications prepared by the compression molding method, *Polym. Compos.,* 45(9), 8104–8118(2024). https://doi.org/10.1002/pc.28327

Nautiyal, S., Dimri, S., Riyal, I., Sharma, H. and Dwivedi, C., Natural fibres and their composites: a review of chemical composition, properties, retting methods, and industrial applications, *Cellul.,* 32(6), 3497–3527(2025). https://doi.org/10.1007/s10570-025-06487-x

Reddy, P. V, Reddy, R. M., Rao, P. S., Krishnudu, D. M., Reddy, R. V. S. and Kumar, A. E., Parameters Selection for Enhanced Mechanical and Wear Properties of Natural Fiber Reinforced Hybrid Composites Using PSI Technique, *J. Nat. Fibers.*, 19(15), 10111–10125(2022). http://dx.doi.org/10.1016/j.matpr.2021.12.043

Rout, I., Singh, M., Mahapatra, T. R., Mishra, P., Dash, S. and Mishra, D., Characterization and Optimization of Dry Sliding Wear Properties of Partially Biodegradable Hybrid Polymer Composites, *J. Bio. Tribo. Corros.,* 11(2), 59(2025). https://doi.org/10.1007/s40735-025-00979-w

Sathiyamurthy, S., Saravanakumar, S., Ananthi, N. and Devi, P., Optimization of fiber length and filler content for improving the mechanical behaviour of musa acuminate fiber-reinforced epoxy composite using response surface methodology, *J. Ceram. Proc. Res.,* 24(4), 683–692(2023). https://doi.org/10.36410/jcpr.2023.24.4.683

Senguptaa, S., Effect of different lignocellulosic fibre-based needle punched nonwovens on mechanical properties of bio-reinforced composite, *Indian. J. Fibre. Text. Res.*, 45(4), 436–443(2020). https://doi.org/10.56042/ijftr.v45i4.31096

Senthilkumar, N., Deepanraj, B., Dhinakarraj, C. K. and Yuvaperiyasamy, M., Characterization Studies on Vetiveria Zizanioides Natural Fiber and Graphene Filler Reinforced Nano Polymer Composite Material, *J. Environ. Nanotechnol.,* 13(2), 214–219(2024). https://doi.org/10.13074/jent.2024.06.242561

Sivanantham, G., Ayyappan, V., Loganathan, P., Mani, S. K., Vijaya, G. S., Raghunathan, V., Rangappa, S. M. and Siengchin, S., Sustainable hybrid composites from flax, vetiver, and Luffa cylindrica: Acoustic and structural performance, *Polym. Compos.,* 1-17(2025). https://doi.org/10.1002/pc.29900

Tavadi, A., Basheer, D., Melese, K. G., Kumaresan, K., Mohan, N., Kerur, M. R. H. and Shashidhara, L. C., Experimental analysis of mechanical properties and FTIR analysis of areca fiber-reinforced epoxy composites incorporating Al_2O_3, *J. Ind. Text.,* 55, 15280837241313217(2025). https://doi.org/10.1177/15280837241313217

Thangaraj, S., Pradeep, G. M., Heaven Dani, M. S., Mayakannan, S. and Benham, A., Experimental investigations on tensile and compressive properties of nano alumina and arecanut shell powder reinforced polypropylene hybrid composites, *Mater. Today. Proc.*, 68, 2243–2248(2022). https://doi.org/10.1007/s10751-024-02121-7

Tyagi, A., Gupta, B. L., Mukhija, L., Bhandari, M., Meena, A. and Meena, S. L., Mechanical and tribological behavior of NFRC's: A comprehensive analysis of properties & applications, *Green. Mater.*, 1-12(2024). https://doi.org/10.1680/jgrma.24.00113

Venkatesh, R., Angalaparameswari, C., Ammaiappan, M., Das, A. D., Arunkumar, G., Kamatchi, R. M. and Kaliyaperumal, G., Effective Utilization of Bast Fiber in High Density Polyethylene Nanocomposite Enriched by Alumina Nanoparticle: Mechanical Performance Evaluation, *J. Inst. Eng. India. Ser. D.*, (2024). https://doi.org/10.1007/s40033-024-00678-9